

Inverse magnetoresistance in magnetic tunnel junction with a plasma-oxidized Fe electrode and the effect of annealing on its transport properties

Chando Park,^{a)} Jian-Gang Zhu, Yingguo Peng, David E. Laughlin, and Robert M. White
Data Storage Systems Center, Carnegie Mellon University, Pittsburgh, Pennsylvania 15213

(Presented on 10 November 2004; published online 5 May 2005)

To understand the transport properties of Fe₃O₄ based magnetic tunnel junctions (MTJ), MTJs with a Fe₃O₄ electrode prepared by *in situ* plasma oxidation of a thin Fe film have been fabricated on oxidized silicon wafers with standard photolithography. High resolution transmission electron microscopy (HRTEM) was used to investigate the interface of the MTJs, and the magnetic and electrical transport properties of the MTJs were measured at different temperatures. TEM cross-section micrographs showed that the plasma oxidized Fe layer was directly in contact with the tunnel barrier (AlO_x), giving the predicted inverse magnetoresistance (MR). As the temperature was lowered, asymmetry in the MR and magnetic hysteresis (MH) curves appeared. A thin FeO phase at the interface seemed to produce this asymmetry. The effects of annealing on the transport properties are also discussed. © 2005 American Institute of Physics. [DOI: 10.1063/1.1850332]

I. INTRODUCTION

As a result of their high spin polarization (100%), half-metallic materials having only one spin subband at the Fermi level are very attractive as electrodes in magnetic tunnel junctions (MTJ). From band calculations, Fe₃O₄ (magnetite) is one of the half metals that has an energy gap in the majority spin band at the Fermi level.¹ There are several methods for fabricating Fe₃O₄ such as reactive sputtering, direct deposition and *in situ* oxidation of deposited Fe.²⁻⁷ For application as an electrode of a MTJ, *in situ* plasma oxidation of deposited Fe has advantages, such as avoiding the interface reaction that occurs at the interface with Al.⁵ In addition, the thickness of Fe₃O₄ formed by this method can be thin enough that the coercivity can be controlled by strong coupling with an adjacent ferromagnet.^{6,7} Recently, we demonstrated the inverse magnetoresistance (MR) of a Fe₃O₄ based MTJ using *in situ* plasma oxidation of deposited Fe, indicating negative spin polarization of Fe₃O₄ in contact with an AlO_x barrier.⁸ Negative spin polarization of Fe₃O₄ in contact with the AlO_x barrier also has been observed by Panchular.⁹ Since bulk Fe₃O₄ has unique electrical properties such as the Verwey transition¹⁰ where the resistance increases nearly two orders of magnitude, measurements of magnetic and electrical properties at low temperature are very important for the understanding of the transport behavior of Fe₃O₄.

In this study, we report on transport and magnetic properties of MTJs with plasma oxidized Fe/AlO_x/NiFe in the temperature range from 60 to 300 K.

II. EXPERIMENT

Magnetic tunnel junctions with the structure of Ta 3 nm/Cu 50 nm/Ta 3 nm/NiFe 10 nm/AlO_x 2 nm/Fe 1.6 nm+oxidation/Fe 10 nm/Ta 3 nm were deposited on

oxidized silicon substrates by using a rf/dc sputtering system. All of our junctions were patterned by photolithography and ion beam etching. The junction sizes varied from 4 × 4 to 16 × 16 μm². The tunnel barrier layer was formed by plasma oxidation of 1.7 nm of Al for 45 s. To obtain the Fe₃O₄ film, we first deposited very thin Fe (1.6 nm) on top of the AlO_x and subsequently oxidized the Fe with an oxygen plasma to produce Fe₃O₄, which was directly in contact with the AlO_x barrier. Another Fe layer was deposited on top of the oxidized Fe layer in order to control the switching of the very thin Fe₃O₄ through its strong exchange coupling with the Fe film. This is accomplished without destroying the Fe₃O₄ phase, which might be caused by its reduction that occurs with other capping layers such as Ta or Al.⁵ The interface of the films was investigated by high resolution transmission electron microscopy (HRTEM), and the magnetic properties were measured at different temperatures using a vibrating sample magnetometer (VSM) using fields up to 500 Oe. The magnetoresistance (MR) transfer curve was measured using a four-point probe measurement system with fields up to 350 Oe.

III. RESULTS AND DISCUSSION

Figure 1 shows cross-section TEM and HRTEM images

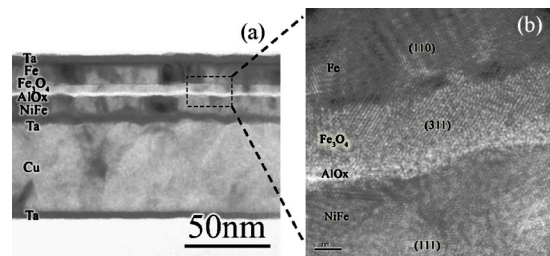


FIG. 1. Cross-section TEM (a), and HRTEM images (b) of the structure of Ta 3 nm/NiFe 10 nm/AlO_x 2 nm/Fe 1.6 nm+O₂ plasma/Fe 10 nm/Ta 3 nm. The inset box indicates the position at which the high-resolution image is taken.

^{a)}Electronic mail: chando@andrew.cmu.edu

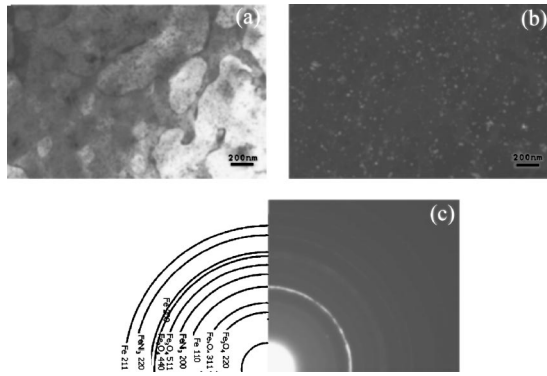


FIG. 2. Bright-field (a) and dark-field (b) images and selected area electron diffraction pattern (c) of the Fe_3O_4 layer in the structure of Ta 3 nm/ Cu 50 nm/ Ta 3 nm/ NiFe 10 nm/ AlO_x 2 nm/ Fe 1.6 nm + O_2 plasma/ Fe 5 nm/ Ta 3 nm.

of the structure of Ta 3 nm/ Cu 50 nm/ Ta 3 nm/ NiFe 10 nm/ AlO_x 2 nm/ Fe 1.6 nm + O_2 plasma/ Fe 10 nm/ Ta 3 nm. To avoid the geometric effect of a nonuniform current distribution,¹¹ a thick layer of Cu (50 nm), as shown in Fig. 1(a), was used as an underlayer. The AlO_x barrier in the cross section TEM image is formed conformally over the NiFe surface. The uniform Fe oxide layer is directly in contact with the AlO_x barrier and its thickness is around 3 nm. To identify the phases in the HRTEM image, we measured the d spacings from the fast Fourier transformation (FFT) of the high-resolution image.^{2,5} The HRTEM image in Fig. 1(b) shows that the phase of the Fe oxide formed by our *in situ* plasma oxidation is Fe_3O_4 . A Fe_3O_4 grain, which displays the (311) crystallographic planes, is shown in the figure. The interface between the top Fe and Fe_3O_4 is very clear and sharp, whereas the interface between Fe_3O_4 and the bottom AlO_x is not sharp, as is shown in the HRTEM image in Fig. 1(b).

The Fe_3O_4 layer formed from the oxidized Fe layer is also identified in the electron diffraction pattern of the plan view TEM image of the Fe_3O_4 layer in the structures of Ta 3 nm/ NiFe 10 nm/ AlO_x 2 nm/ Fe 1.6 nm + O_2 plasma/ Fe 5 nm/ Ta 3 nm, as shown in Fig. 2(c). To make a sample for the TEM plan view image of the Fe_3O_4 layer, an ion milling step was precisely controlled to produce a thin area of the Fe_3O_4 layer in a sample with multilayers. The diffraction rings clearly indicate the Fe_3O_4 phase along with Fe and FeNi_3 phases that are associated with the top and the bottom electrode, respectively. The bright- and dark-field images [Figs. 2(a) and 2(b)] show grain sizes in the range of 5–10 nm with no apparent texture.

Figure 3 shows the magnetoresistance (MR) transfer curves of a MTJ with the structure of Ta 3 nm/ Cu 50 nm/ Ta 3 nm/ NiFe 10 nm/ AlO_x 2 nm/ Fe 1.6 nm + O_2 plasma/ Fe 10 nm/ Ta 3 nm, and a junction size of $16 \times 12 \mu\text{m}^2$. All MRs were inverse at the temperatures measured, as expected since the polarization of Fe_3O_4 and NiFe with the AlO_x barrier is negative and positive, respectively. As the temperature decreased, the magnitude of the MR, the switching field and the junction resistance increased. The switching field of the Fe oxide increased more than twice between 300 and 60 K while the switching field of NiFe remained about the same.

For example, if we define the switching field where switching occurs above 90%, the switching field of Fe oxide changed from 65 Oe at room temperature to 145 Oe at 60 K. It has been reported that spin polarization increases with decreasing temperature.¹² The increase in junction magnetoresistance (JMR) from -1.2% to -2.75% is believed to be due to both the increase of spin polarization of NiFe and plasma oxidized Fe at low temperature. The switching field is related to the anisotropy constant of Fe_3O_4 , which has a strong temperature dependence.¹³ A reference MTJ (Fe/ AlO_x / NiFe) with the same structure as the plasma oxidized Fe based tunnel junction except for the plasma oxidized Fe layer, shows an increase in resistance of $\sim 10\%$ (not shown). The large increase ($\sim 120\%$) in resistance upon cooling, shown in Fig. 3, is therefore due to the iron oxide layer in the MTJ. However, the exponential increase in resistance with decreasing temperature, which has been observed in Fe_3O_4 ,¹⁰ was not seen here probably because the Fe oxide layer is so thin (~ 3 nm) that the resistance of this layer is much less than that of tunnel barrier (AlO_x). Only at low temperature, is the resistance of the iron oxide layer comparable to that of the tunnel barrier, resulting in a much larger increase in junction resistance. One interesting observation is the asymmetry occurring in the MR curve at low temperature. At room temperature, the MR curve was symmetric. The asymmetry in the MR curve is thought to be related to the interface composition between the Fe oxide layer and the AlO_x barrier. The phase at the interface can be a mixture of ferrimagnetic (Fe_3O_4) and antiferromagnetic phases (FeO or $\alpha\text{-Fe}_2\text{O}_3$) which can cause a shift in the MR curve. FeO and $\alpha\text{-Fe}_2\text{O}_3$ have Néel temperatures of ~ 198 K and 973 K, respectively.^{14,15} Since there is no asymmetry at room temperature, the antiferromagnetic material is most likely FeO because FeO acts as a paramagnet at room temperature. However, we cannot detect the FeO phase in an HRTEM image (Fig. 1), indicating that it must be a very thin layer. Amorphous AlO_x might blur the interface so that we cannot distinguish the FeO phase from Fe_3O_4 . One recent report showed that from first principle calculations on the tunnel junction structure of Fe–FeO–MgO–Fe, a single atomic iron oxide layer (FeO) between the electrode and the tunnel barrier can change the conductance by more than an order of magnitude, resulting in a greatly reduced MR.¹⁶ Therefore, the reason that the magnitude of MR in our junction is much smaller than expected could be due to a small amount of FeO at the interface. It is important to note the possibility that the asymmetry in the MR curve is due to pure Fe_3O_4 itself because Fe– Fe_3O_4 bilayer films as well as single layer Fe_3O_4 films has been reported to produce shifted hysteresis loops at low temperatures.^{17,18}

To confirm whether FeO exists or not, magnetic hysteresis loops of an unpatterned MTJ composed of Ta 3 nm/ Cu 50 nm/ Ta 3 nm/ NiFe 10 nm/ AlO_x 2 nm/ Fe 1.6 nm + O_2 plasma/ Fe 10 nm/ Ta 3 nm were measured at room temperature and low temperature (300, 210, and 110 K). Figure 4 shows the MH loops measured for our MTJ structure. The MH loops contained two sub loops for NiFe and Fe oxide coupled with Fe. At 300 and 210 K, there was no shift in the loop while there was about 10 Oe shift in the loop at

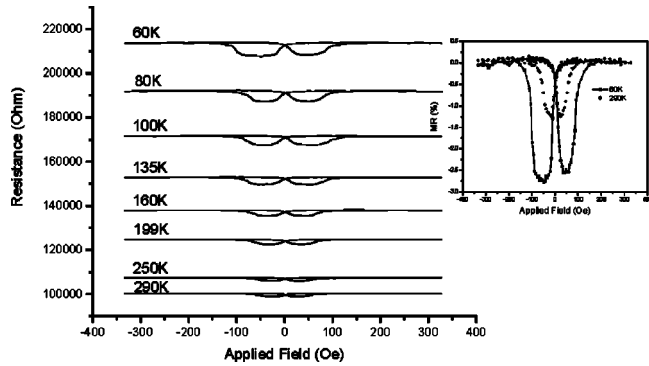


FIG. 3. Magnetoresistance transfer curves of the junction structure of Ta 3 nm/Cu 50 nm/Ta 3 nm/NiFe 10 nm/ AlO_x 2 nm/Fe 1.6 nm+ O_2 plasma/Fe 10 nm/Ta 3 nm as a function of temperature. Inset in the upper corner shows MR curves at 60 and 290 K.

110 K. The shift only occurred in the subloop for Fe oxide coupled with Fe, but not in the loop for NiFe. This suggests the existence of the FeO phase in the Fe oxide electrode of our MTJ structure, which is consistent with the MR curves shown in Fig. 3. The coercivities of these MH loops are well matched with the switching fields of the MR curve.

Figure 5 shows the MR transfer curves of the MTJ before and after annealing at 150 °C for 3 h. Since the FeO phase is unstable below 570 K and decomposes into Fe + Fe_3O_4 at low temperature,¹⁹ an annealing treatment can remove the FeO phase.² As shown in Fig 5, the MR changed from being inverse to being positive after annealing. We believe that this reaction [$4\text{FeO} \rightarrow \text{Fe}_3\text{O}_4 + \text{Fe}$, $\Delta G = -34\,816.3$ J at 300 K (Ref. 20)] occurs at the interface during annealing, resulting in the positive MR. Previous results also show that if there is a small amount of Fe, a positive MR appears.⁸ Therefore, our results suggest that relatively low MR comes from the FeO phase at the interface even though Fe_3O_4 coexists with FeO at the interface. In our case, the contribution from the FeO phase at the interface may be significant.

IV. SUMMARY

We have studied the behavior of a magnetic tunnel junction having Fe_3O_4 as one of the electrodes. The existence of

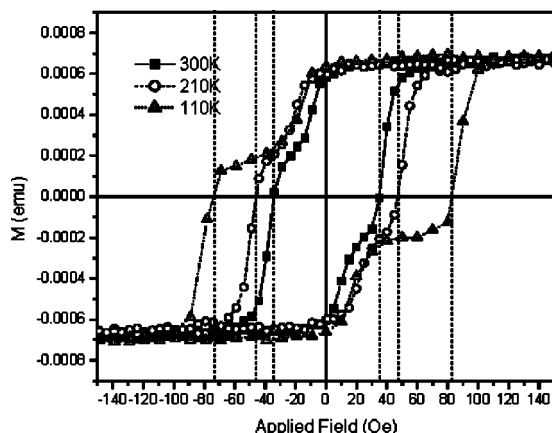


FIG. 4. Magnetic hysteresis loops of the junction structure of Ta 3 nm/Cu 50 nm/Ta 3 nm/NiFe 10 nm/ AlO_x 2 nm/Fe 1.6 nm+ O_2 plasma/Fe 10 nm/Ta 3 nm at temperature of 300, 210 and 110 K. The junction was cooled in the presence of a magnetic field (10 000 Oe).

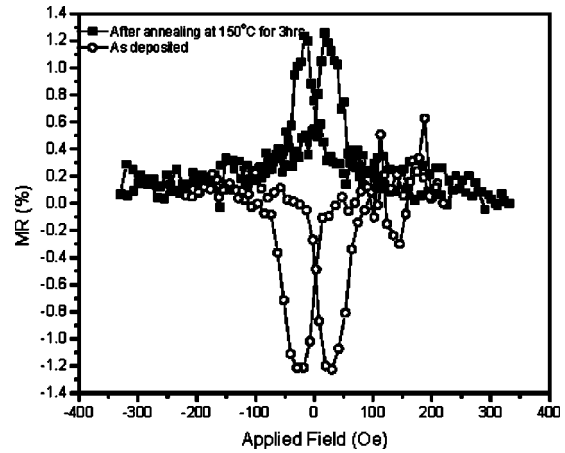


FIG. 5. Magnetoresistance transfer curves of junction structure of Ta 3 nm/Cu 50 nm/Ta 3 nm/NiFe 10 nm/ AlO_x 2 nm/Fe 1.6 nm+ O_2 plasma/Fe 10 nm/Ta 3 nm before annealing and after annealing at 150 °C for 3 h.

FeO at the interface between the AlO_x and the Fe oxide not only induces asymmetry in the MR curve at low temperature, but also causes the poor transport properties of the Fe_3O_4 based magnetic tunnel junction.

ACKNOWLEDGMENT

The authors gratefully acknowledge the Data Storage Systems Center for its financial support of the research project.

- ¹Z. Zhang and S. Satpathy, Phys. Rev. B **44**, 13319 (1991).
- ²C. Park, Y. Shi, Y. Peng, K. Barmark, J. G. Zhu, D. E. Laughlin, and R. M. White, IEEE Trans. Magn. **39**, 2806 (2003).
- ³Y. Peng, C. Park, and D. E. Laughlin, J. Appl. Phys. **93**, 7957 (2003).
- ⁴M. Fonin, Yu. S. Dedkov, J. Mayer, U. Rüdiger, and G. Güntherodt, Phys. Rev. B **68**, 045414 (2003).
- ⁵Y. Peng, C. Park, J. G. Zhu, R. M. White, and D. E. Laughlin, J. Appl. Phys. **95**, 6798 (2004).
- ⁶E. Snoeck, V. Serin, R. Fourmeaux, Z. Zhang, and P. P. Freitas, J. Appl. Phys. **96**, 3307 (2004).
- ⁷Z. Zhang, S. Cardoso, P. P. Freitas, P. Wei, N. Barradas, and J. C. Soares, Appl. Phys. Lett. **78**, 2911 (2001).
- ⁸C. Park, Y. Peng, J. G. Zhu, D. E. Laughlin, and R. M. White (unpublished).
- ⁹A. Panchular, Ph.D. dissertation, Stanford University, 2003.
- ¹⁰E. J. W. Verwey, Nature (London) **144**, 327 (1939).
- ¹¹J. S. Moodera, L. R. Kinder, J. Nowak, P. LeClair, and R. Meservey, Appl. Phys. Lett. **69**, 708 (1996).
- ¹²C. H. Shang, J. Nowak, R. Jansen, and J. S. Moodera, Phys. Rev. B **58**, R2917 (1998).
- ¹³K. Abe, Y. Miyamoto, and S. Chikazumi, J. Phys. Soc. Jpn. **41**, 1894 (1976).
- ¹⁴M. S. Seehra and G. Srinivasan, J. Phys. C **17**, 883 (1984).
- ¹⁵A. H. Morrish, *Canted Antiferromagnetism: Hematite* (World Scientific, Singapore, 1994), p. 52.
- ¹⁶X.-G. Zhang, W. H. Butler, and A. Bandyopadhyay, Phys. Rev. B **68**, 092402 (2003).
- ¹⁷D. V. Dimitrov, A. S. Murthy, G. C. Hadjipanayis, and C. P. Swann, J. Appl. Phys. **79**, 5106 (1996).
- ¹⁸D. T. Margulies, F. T. Parker, F. E. Spada, R. S. Goldman, J. Li, R. Sinclair, and A. E. Berkowitz, Phys. Rev. B **53**, 9175 (1996).
- ¹⁹T. B. Massalski, *Binary Alloy Phase Diagrams* (ASM International, Materials Park, OH, 1990), Vol. 2, p. 1739.
- ²⁰T. B. Reed, *Free Energy of Formation of Binary Compounds: An Atlas of Charts For High-Temperature Chemical Calculations* (MIT Press, Cambridge, MA, 1971).